

Simulation and testing of a graded negative index of refraction lens

R. B. Greegor, C. G. Parazzoli, J. A. Nielsen, M. A. Thompson, and M. H. Tanielian
Boeing Phantom Works, Seattle, Washington 98124

D. R. Smith
Duke University, Durham, North Carolina 27706

(Received 26 January 2005; accepted 11 July 2005; published online 25 August 2005)

A gradient index (GRIN) lens using a negative index of refraction material (NIM) has been designed and tested. The GRIN lens was fabricated using a NIM slab with a variable index of refraction perpendicular to the propagation direction. Ray tracing calculations based on the isotropic Eikonal equation determined the index of refraction gradient required for a given focal length. An electromagnetic code was then used to design the required ring and wire unit cells. Finally, the index of refraction was approximated using ten discrete steps in an effective medium simulation for the GRIN lens that agreed with the experimental measurements. © 2005 American Institute of Physics. [DOI: 10.1063/1.2037202]

Negative index of refraction materials (NIM) were first postulated by Veselago¹ and have been realized recently in the GHz region using rings and wires patterned on circuit boards.^{2,3} The ring and wire approach has been used to create Snell's Law wedges^{3,4} as well as lenses⁵ having curved surfaces approximated using steps that are multiples of the NIM unit cell dimension. Flat gradient index (GRIN) lenses using positive index materials are common,⁶ but only recently have they been suggested having metamaterial elements.⁷

In the following, we report the design and testing of a GRIN lens based on unit cells composed of rings and wires. The absolute sign of the index does not enter into consideration, at least in a first approximation. However, the general dispersion characteristics associated with NIM structures make the NIM unit cell a convenient starting point for the GRIN structure. Also, the larger range of material response available in metamaterials should lead to improved GRIN lens design. In particular, since the permittivity and permeability of a metamaterial can be adjusted independently, metamaterial GRIN lenses can presumably be better matched to free space.

The GRIN lens is constructed by using a slab of NIM with a variable index of refraction in the y direction, perpendicular to the direction of propagation z . The principle advantage of a GRIN lens is its uniform thickness, which on average is thinner than a curved constant index of refraction lens as shown in Fig. 1 for GRIN ($n=-1.0$ to -2.6), NIM ($n=-1.0$), and positive index material (PIM) ($n=2.0$) lenses of 5.4 cm focal length. The thickness used for the GRIN lens is five NIM unit cells in the propagation direction. This thickness is less than the wavelength of the incident electromagnetic radiation at ~ 17 GHz used to test the lens, reducing the transmission losses and potentially producing higher quality images.

To design the GRIN lens we used ray-tracing calculations based on the isotropic Eikonal equation⁸ to determine the index of refraction dependence required for a given focal length GRIN lens. This approach is only an approximation because our NIM material is not fully isotropic. The isotropic Eikonal equation has the form

$$\frac{d}{ds} \left(n \frac{d\vec{r}}{ds} \right) = \nabla n,$$

where n is the index of refraction of the isotropic material and s is the arc length along the ray. It is convenient to make the following assumption for the refractive index:

$$n(y) = n_0 + n_2 y^2.$$

This form of the index of refraction is sufficient for our purposes. Substitution of $n(y)$ in the Eikonal equation yields a set of ODE's that can be solved numerically. The constants n_0 and n_2 are empirically adjusted to achieve the desired focal length. The index of refraction profile shown in Fig. 2(a) is for $n(y) = n_0 + n_2 y^2$, where $n_0 = -1.0$ and $n_2 = -0.07$. We approximated the index profile with a ten step staircase (dashed line) starting and ending at multiples of the unit cell dimension (2.510 mm). To obtain a sharper image, higher order terms are needed for the index of refraction dependence on y , along with finer steps in the index of refraction profile. However, finer step sizes are not achievable at this time given the tolerances associated with our fabrication process. Ray tracing analysis shown in Fig. 2(b) was done using

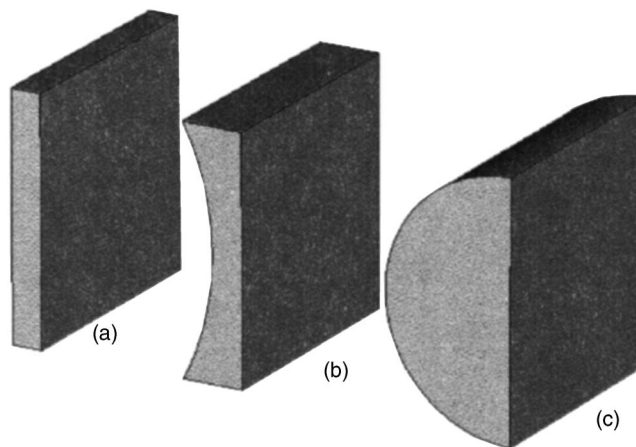


FIG. 1. Lens size and shape for (a) GRIN ($n=-1.0$ to -2.6), (b) NIM ($n=-1.0$), and (c) positive index material (PIM) ($n=2.0$) lenses of 5.4 cm focal length. Note that a GRIN lens is smaller than comparable NIM and PIM lenses.

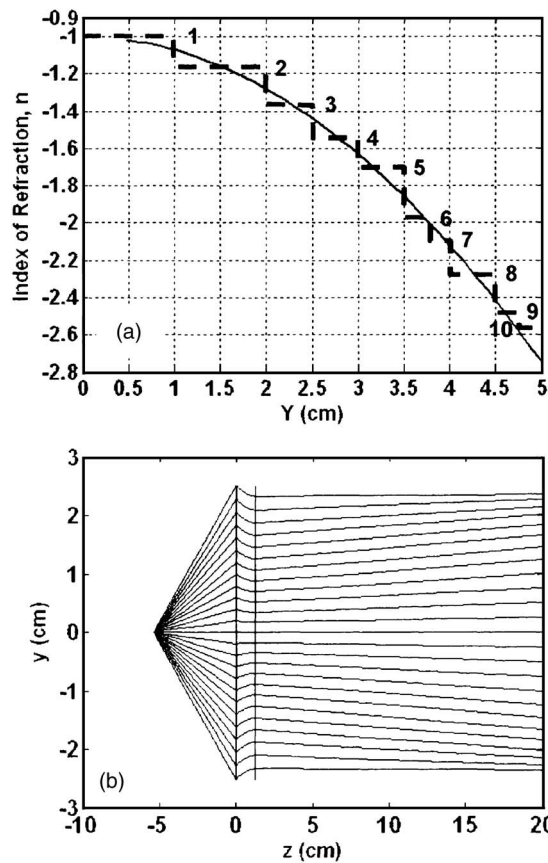


FIG. 2. (a) Index of refraction and discretization (dashed line) used for GRIN lens. (b) Ray tracing using Eikonal equation having smooth index profile shown in (a).

the Eikonal equation with the smooth index profile shown in Fig. 2(a). The resulting focal length of the lens is approximately 5.4 cm from the first surface of the lens giving an F number of ~ 1.1 for a lens diameter of 5.0 cm.

Having determined the required $n(y)$ for the GRIN lens, an electromagnetic code Microwave Studio (MWS)⁹ employed previously in Ref. 5 was then used to design the ring and wire unit cell structure having the desired refractive index y dependence. A unit cell having $n = -1.0$, utilizing copper patterns on a Rogers 5880 substrate and Rohacell foam filling the void is shown in Fig. 3. The values for the $n = -1.0$ unit cell parameters are: 2.510 mm cubic unit cell, 0.015 mm ring gap, 0.300 mm ring wire width, 2.000 mm ring length along the outer side, and 0.100 mm wire width. The ring gap, ring width, side length of ring, and wire width

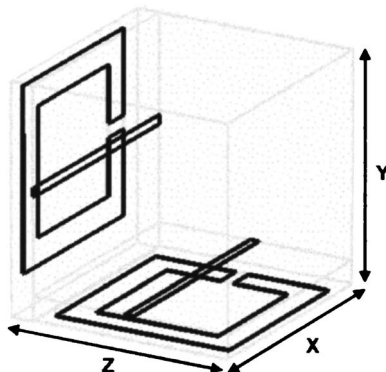


FIG. 3. Unit cell design geometry for GRIN lens.

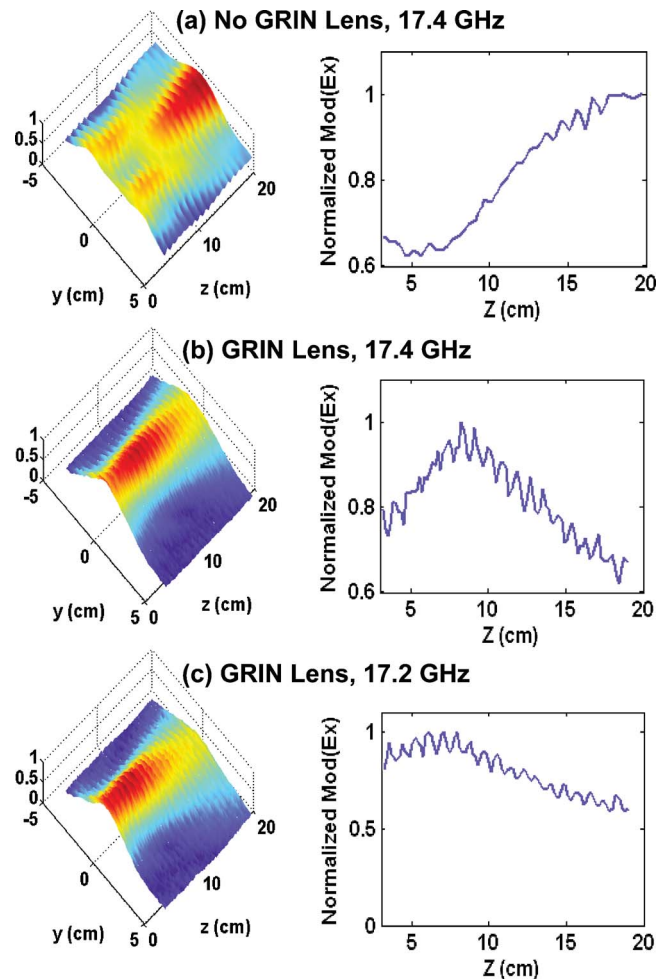


FIG. 4. (Color) Approximate plane wave illuminated normalized experimental $|E_x|$ contours with and without GRIN lens at 17.2 and 17.4 GHz.

of this unit cell were multiplied by a fraction f having values of 1.00, 0.99, 0.98, 0.97, and 0.96. The scattering parameters for these unit cells were then calculated using MWS from which the index of refraction n , the impedance Z , the permittivity ϵ , and permeability μ were retrieved. The retrieved values of n and Z at ~ 17.0 GHz were plotted as a function of f . From this figure the required values of f were determined corresponding to the ten steps in the index of refraction profile shown in Fig. 2(a). The n values ranged from approximately -1.0 to -2.6 and the Z values were 1.00 ± 0.300 . Multiple unit cells were arranged in a manner to produce a flat GRIN lens having dimensions of approximately $x = 127$ mm, $y = 100$ mm, and $z = 12.5$ mm.

The E_x field pattern of the flat GRIN lens was simulated using MWS for both point source and plane wave illumination. This was accomplished by simulating the rings and wires as an effective medium having ten steps in the index of refraction along the y -axis as shown in Fig. 2(a). The negative index was modeled in MWS using the Lorentz dispersion relation such that at ~ 17.0 GHz the lens would have the desired refractive index at the predetermined y locations. We used the Lorentz dispersion relation

$$\epsilon = \epsilon_h + (\epsilon_s - \epsilon_h) \omega_0^2 / (\omega_0^2 + i2\pi\omega f_d - \omega^2),$$

where ϵ_h is the high frequency relative permittivity, ϵ_s is the relative permittivity at $\omega = 0$, ω_0 is the resonance frequency,

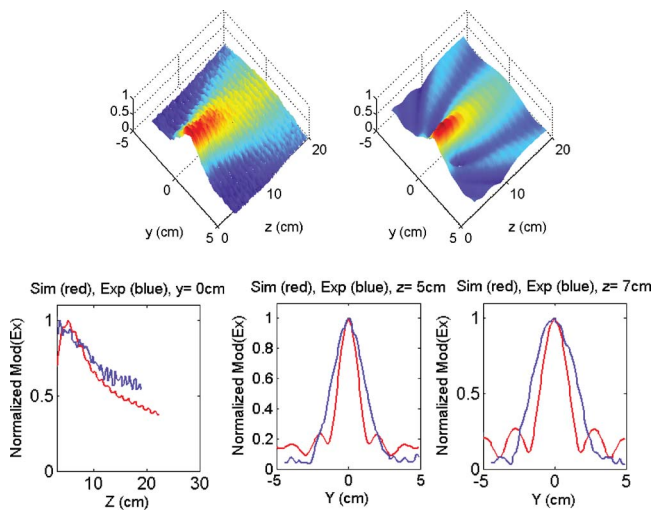


FIG. 5. (Color) Approximate plane wave illuminated normalized experimental (left) and simulated (right) $|E_x|$ surface and line plots (bottom) for GRIN lens at 17.0 GHz. For the line plots the simulated values are shown in red and the measured values in blue.

and f_d is the damping factor. The impedance match was assumed to be $Z=1$, that is $\varepsilon=\mu$.

The plane wave experimental results are shown in Fig. 4 with and without the GRIN lens in place at 17.2 and 17.4 GHz using a horn placed at 150 cm away from the front surface of the lens. This created a diverging electromagnetic beam of approximately six degrees. Figure 5 shows the results of the comparison for the simulated and experimental $|E_x|$ surface and line plots. The results of Fig. 5 locate the focal region of the lens at approximately 5 to 6 cm (at ~ 17 GHz) from the center of the lens in good agreement with the results of the isotropic Eikonal calculations. This justifies the use of the isotropic Eikonal equation for this lens simulation.

These figures clearly show the focusing properties of the GRIN lens and the expected shift in the focal spot closer to the lens for lower frequencies where the NIM index of refraction is higher. Furthermore, we observe that the simulations and experimental results are in reasonable agreement.

In addition to imaging and focusing simulations, we have also performed steering calculations for the flat GRIN lens using our ray tracing algorithm. We accomplished this by moving the source along the y direction from $y=0$ cm to

+1.0 and +2.0 cm at the focal distance of approximately 5.4 cm. This resulted in steering the beam off axis by $\sim 10^\circ$ and $\sim 20^\circ$, respectively. We corroborated this result using a MWS electromagnetic simulation.

In conclusion, we have designed, constructed, and tested a GRIN lens using a NIM slab. The requirements for the gradient in the refractive index were determined using the Eikonal equation. We designed NIM ring and wire unit cells to match this profile using an electromagnetic code (MWS). The smooth profile was approximated using ten discretized steps each having unique NIM unit cell parameters. The flat GRIN lens was constructed using these unit cells and measurements were made and compared to effective medium simulations. We found reasonable agreement between our predictions and measurements, demonstrating the efficacy of using NIM slabs to construct a GRIN lens. Such a flat lens has lower losses since it is thinner than curved surface NIM lenses and, hence, can also potentially produce sharper focusing and improved imaging characteristics. In addition, since the permittivity and permeability can be controlled separately in metamaterials, the index $(\varepsilon\mu)^{1/2}$ can be varied while maintaining the impedance $(\mu/\varepsilon)^{1/2}$ nearly constant. As we have demonstrated here, this feature allows large gradients to be utilized while maintaining good match across the entire lens.

This work was supported by DARPA Contract MDA972-01-2-0016. We acknowledge D. Schurig, S. Schultz, and D.C. Vier for useful suggestions and discussions.

¹V. G. Veselago, *Sov. Phys. Usp.* **10**, 509 (1968).

²D. R. Smith, W. Padilla, D. C. Vier, S. C. Nemat-Nasser, and S. Schultz, *Phys. Rev. Lett.* **84**, 4184 (2000).

³R. A. Shelby, D. R. Smith, and S. Schultz, *Science* **292**, 77 (2001).

⁴C. G. Parazzoli, R. B. Greeger, K. Li, B. E. C. Koltenbah, and M. H. Tanielian, *Phys. Rev. Lett.* **90**, 107001 (2003).

⁵C. G. Parazzoli, R. B. Greeger, J. A. Nielsen, M. A. Thompson, K. Li, A. M. Vetter, and M. H. Tanielian, *Appl. Phys. Lett.* **84**, 3232 (2004).

⁶See, for example, E. W. Marchand, *Gradient Index Optics* (Academic, London, 1978).

⁷D. R. Smith, J. J. Mock, A. F. Starr, and D. Schurig, *Phys. Rev. E* **71**, 036609 (2005).

⁸L. B. Felsen and N. Marcuvitz, *Radiation and Scattering of Waves* (Prentice-Hall, Englewood Cliffs, N.J., 1973), Chap. 1.

⁹Microwave Studio is a registered trademark of Computer Simulation Technology (CST), GmbH, Darmstadt, Germany.